Using Mean-Squared-Error in Log-Transformed Domain to Evaluate Speckle Filters.

Thanh-Hai Le, Ian McLoughlin, Quang-Huy Nguyen, Chan-Hua Vun

***Abstract*—Logarithmic transformation has the potential to convert the multiplicative and heteroskedastic statistical distribution of SAR speckle noise into a simpler additive and homoskedastic distribution model. From this homoskedastic model, within the log-transformed domain, a few consistent measures of distance emerge. With these, subtractive differences become consistent and predictable. We show, through experiments and analysis, that the familiar mean-squared-error (MSE) criteria can reliably serve as a single unifying performance indicator to evaluate SAR speckle filters. In homogeneous areas, we establish a mathematical relationship that links the variance of log-transformed SAR data with the canonical Equivalent-Number-of-Looks index. For heterogeneous scenes, the standard residual-based bias evaluation, also in the log-transformed domain, is shown to be equivalent to the ratio-based radiometric preservation criteria, frequently employed in the original domain. Through experiments as well as analysis, we show that lower MSE suggests better feature detection and classification ability, which can be an important requirement for subsequent post-filtering steps in practical SAR data processing. Combining bias and variance evaluation, we propose and describe the use of MSE evaluation in log-transformed domain to evaluate SAR speckle filters.**

***Index Terms*—Synthetic aperture radar, speckle-filtering, homoskedasticity, mean-squared-error**

I. Introduction

The nature of SAR speckle is that it is stochastic even if the underlying radiometry is constant. And when there are spatial radiometric variation, not only its expected value changes, its heteroskedastic variance varies as well. Nevertheless, statistical models have been developed to derive the underlying back-scattering coefficient (σ) from measured SAR data. As such, speckle filters are, by and large, estimators that attempt to determine this unknown coefficient from observable SAR data.

SAR speckle-filtering can be, and has been, positioned within the context of estimation theory [1]. The stages in this statistical framework consist of statistical modeling, estimator development and evaluation of the estimators' performance. Estimators are typically evaluated based on the bias and variance properties of their estimates: lower bias and/or lower variance would lead to lower MSE, which then indicates better accuracy. Ideally, estimator evaluation should be based both qualitatively on some real data and quantitatively through simulated experiments. In addition, due to the stochastic nature of SAR-processing, and thus its simulating process, statistical summaries of repeatedly-simulated experiments are normally preferred to single-run results.

Our survey of SAR speckle filter research, however, indicates a different picture from the standard practice of the statistical framework, specifically, in the stage of performance evaluation. Due to the multiplicative and heteroskedastic nature of speckle noise, bias and variance evaluation may not be the most useful measures. Thus, the standard evaluation metric of mean-squared-error is not easily applicable, prompting alternative evaluation criteria to be proposed. In fact, our survey of relevant literature fails to reveal a single universally agreed quantitative metric for the performance of speckle filters.

Most commonly, each newly proposed speckle filter tends to be published along with its own methodology for evaluating its performance. As such, many papers lack a comparative basis beyond simple visual qualitative comparison on a few image scenes. While such visual comparison is useful, as an evaluative methodology, regrettably it lacks scientific objectivity. Some papers do present quantitative measurements. However, due to the lack of a standardized performance criteria, the evaluation metrics can change significantly from one paper to the next.

In this paper, we propose and validate the use of MSE in the homoskedastic log-transformed domain to evaluate speckle filters. The paper is structured as follows. Section II briefly surveys related work in the published literature, Section III provides a brief discussion of the logarithmic transformation. Section IV then illustrates the use of variance (an MSE component) in the log-transformed domain to evaluate different filters' speckle suppression power over homogeneous areas. Section V describes the use of the same MSE to evaluate the performance of speckle filters in heterogeneous areas. Section VI hypothesizes the use of residual MSE in the log-transformed domain as a criteria for choosing the most suitable speckle filter for a given satellite-captured SAR image. Finally, Section VII discusses the findings and presents concluding remarks.

II. Related Work in Literature

It is customary to divide the performance evaluation of speckle filters into two distinct classes of homogeneous and heterogeneous region evaluation. Across homogeneous areas, speckle filters are expected to estimate with negligible radiometric bias. As such, evaluating speckle filters over homogeneous areas has traditionally been focused on evaluating

Thanh-Hai Le, Quang-Huy Nguyen and Chan-Hua Vun are with School of Computer Engineering, Nanyang Technological University, Singapore. Ian McLoughlin is with School of Information Science and Technology, University of Science and Technology of China.

The authors wish to thank Dr. Ken-Yoong Lee and Dr. Timo Brestchneider of EADS Innovation-Works Singapore for their initial discussions and for providing us the RADAR-SAT2 imagery used in this paper.

Manuscript received ?, 2012; revised ?.

the variation of the estimators' output (a.k.a the speckle suppression power). In contrast, the methodologies used to evaluate speckle filters over heterogeneous areas are much more complicated, due in part to the following difficulties. The first is that of determining an absolute ground-truth against which quantitative criteria can be measured. The second challenge is to then define a quantifiable metric that allows the performance of different speckle filters to be measured and compared.

In general, any metric to evaluate speckle filters should be relevant to the normal usage of such filters. Furthermore, the application of any speckle filter in a SAR processing framework should enable an improvement in the measurement, detection or classification of the underlying radiometric features. As shown in the subsequent sections, by applying log-transformation, this overall requirement of speckle filtering can be further broken down into two smaller requirements. On the one hand, speckle filters should preserve the underlying radiometric signal (namely the radiometric preservation requirement). On the other hand, they should reduce the variation of the additive noise (i.e. speckle suppression power). These requirements can be measured and evaluated by determining, also in the log-transformed domain, the bias and variance error of the output. As the MSE evaluation is a combination of bias and variance error, it is therefore capable of evaluating the general requirements of speckle filtering.

For homogeneous scenes where the underlying radiometry is assumed to be constant, the filtered results are considered, statistically speaking, to be samples of a single but complex stochastic process. From a logarithmic transformation perspective, the radiometric preservation and speckle suppression requirements of speckle filters can be judged using the familiar bias and variance evaluation.

One metric that can be used to detect radiometric distortion is the ratio between the estimated and the original value $r = X_{est}/X_{org}$ [2] [3]. A somewhat similar metric is used in [4] as $r_w = (X_{est} - X_{org})/X_{org}$. In the log-transformed domain, the equivalent criteria for evaluation could be performed by a simple subtraction. In other words, it is clear that the bias evaluation in the log-transformed domain can be used to evaluate the radiometric preservation requirement of speckle filters.

Specifically for homogeneous scenes, Shi et al. [5] found that in the original domain the "standard" filters (boxcar, Lee [6], Kuan [7], Frost [8], MAP [9]) and their enhanced versions [10] can achieve negligible bias. In this paper, we will also show that all of these standard filters preserve not only the expected radiometric values but also a number of subtractive and consistent measures of distance exhibited in the log-transformed domain.

Several metrics have been developed to evaluate speckle suppression power. The most common measure is the Equivalent Number of Looks (ENL) index $ENL = avg(I)^2/var(I)$ that was proposed by Lee [11]. Another very similar metric is the ratio of mean to standard deviation, $R = avg(I)/std(I)$ [12] In Section IV, it will be shown that, for homogeneous areas, ENL is mathematically related to variance in the log-transformed domain. Subsequently, we propose the use of log-variance to evaluate the noise suppression power of speckle filters, which is the primary criteria used to evaluate speckle filters over homogeneous area.

Real-life and practical images, however, are not homogeneous. Thus there are a number of associated difficulties in evaluating speckle filters over heterogeneous scenes. The first difficulty in evaluating speckle filters for heterogeneous scenes is to select the basis for comparison. It is trivially easy to estimate the underlying radiometric coefficient if an area is known to be homogeneous. However, without simulation or access to solid ground-truth, it is practically impossible to do so for real-life images. And hence, the need for speckle filters estimation is warranted.

Without ground truth, one way to evaluate radiometric preservation of filters is to compute the ratio image mentioned above. Under a multiplicative model, the ratio image is expected to comprise solely of the noise being removed (i.e. it should be completely random). Being random, this should display as little "visible" structure as possible. However, when displaying such images for visual evaluation, the ratios that are smaller than unity are much harder to distinguish than those that are bigger [3]. We therefore propose to adopt a log-transformed domain perspective where the multiplicative noise would then be transformed into a more familiar additive model. More importantly, the ratio image would then become a simple subtraction image. The evaluation methodology for such adoption would not change. Only that the residual image would become linear and additive. And thus it would be more natural to be displayed and evaluated visually (see III-F).

Another way to evaluate speckle filters is by comparing the feature preservation characteristics of the original noised data and those of the filtered image. When there is no ground-truth given, the feature are estimated in both the original noised and the filtered images. Evaluation would then determine how closely related the two feature maps are. Various methods may be applied to extract features; examples of those that have been used are the Hough Transform [3], Robert gradient edge detector [12] and edge map [8]. While significant effort has been spent on these evaluations, serious doubts remain concerning the precision of these methodologies. This is because feature extraction algorithms are only approximations, whose accuracy is not only dependent upon the characteristics of the original image but also heavily affected by the inherent noise. Unfortunately, speckle filters invariably alter the noise characteristics. Thus, without a clear understanding of these dependencies and no absolute ground truth, using feature extraction algorithms to evaluate speckle filters would leave serious questions on how to interpret the results, especially its accuracy.

Since SAR statistical models are quite well understood, simulation experiments with known ground-truth can be employed to evaluate speckle filters. In this paper, we also make use of a methodology similar to the ones discussed above with two important changes. Firstly, our simulated experiments offer absolute ground-truth. Secondly, our threshold-based feature extraction algorithm is extremely simple. More importantly, the dependency between the performance of the algorithm and the level of noise is well established. This performance can

be conveniently visualized by plotting the Receiver Operating Characteristics Curve (ROC). It can also be objectively quantified by measuring the Area Under this Curve (AUC). As shown in section V, this standard and normalized criteria allows a comparative evaluation of feature preservation capabilities for different speckle filters.

Even with known ground-truth, evaluating metrics need to be defined for quantitative measurements. This is the second difficulty in evaluating speckle filters for heterogeneous scenes. Under the conditions of heterogeneity, the standard speckle filters still introduce radiometric loss, normally at local or regional levels. In fact, the common consensus is that a powerful speckle suppression filter (for example the boxcar filter) is likely to perform poorly in terms of preserving underlying radiometric differences (e.g. causing excessive blurring). Furthermore, we have not found many published articles combining the evaluation of these two seemingly contradicting requirements.

Overall, many different methods and metrics have been proposed to evaluate various aspects of speckle filters. However it is clearly advantageous to have a single metric that is able to judge if one filter is better than another. Wang [4] proposed using fuzzy membership to weight opinions of an expert panel. Although this provides a potential solution, we consider it to be tedious in implementation, fuzzy in concept and subjective in nature.

Another approach is to apply a universal mean squared error criteria into the context of SAR data. However since SAR data is heteroskedastic, which violates the assumptions of the Gauss-Markov theorem, the use of MSE is not straightforward. Thus Gagnon [12] suggested the use of the ratio between the expected mean of the signal and the RMSE of the removed noise. The metric is argued to be similar in interpretation to the standard signal-to-noise ratio (SNR). Others have suggested the use of normalized MSE, which is essentially the ratio between MSE and the expected mean.

In this paper, homoskedastic property is shown to be available after logarithmic transformation of SAR data. As the important Gauss-Markov theorem becomes applicable in this transformed domain, the use of MSE is shown to be again relevant for evaluating statistical estimators (i.e. speckle filters). Intuitively, each components of the MSE measure, namely bias and variance evaluation, can be mapped into the requirements of radiometric preservation and speckle suppression for speckle filters. Before the details of our evaluation methodology is presented and discussed, Section III provides a brief discussion on logarithmic transformation for SAR images.

III. Logarithmic Transformation

In this section, the SAR speckle model in the original domain is first shown to be multiplicative and heteroskedastic. The impacts of heteroskedasticity on speckle filtering is then discussed. Logarithmic transformation is then shown to convert original speckle data into an homoskedastic model, where the noise is not only additive, but also independent of the underlying radiometric signal. From the consistent and additive noise in log-transformed domain, the consistent measures of dispersion ($ln(I) - ln(avg(I))$), contrast ($ln(I_1) - ln(I_2)$ and variance ($var(ln(I))$) are described.

A. Original Heteroskedastic Model

The SAR speckle phenomena is often explained as the interference of many coherent but dephased back-scattering components, each reflecting from different and distributed elementary scatterers [13], [14]. This interference can be considered as a random walk on the 2D complex plane [15]. The random nature of the process arises due to the unknown random location, height, distance and thus random phase of each elementary scaterer and its response.

Assuming the Central Limit Theorem is applicable [16], the real part A_r as well as the imaginary part A_i of the observed SAR signal A can then be considered as random variables from uncorrelated Gaussian distributed stochastic processes with zero means and identical variances $\sigma^2/2$ [17]. Their probability density function (pdf) is given as:

$$pdf(A_x) = \frac{1}{\sqrt{\pi}\sigma} e^{\left(\frac{A_x^2}{\sigma^2}\right)} \tag{1}$$

It can then be proved that the measurable amplitude $A = \sqrt{A_r^2 + A_i^2}$ is a random variable of Rayleigh distribution and consequently the intensity $I = A^2 = (A_r^2 + A_i^2)$ is a random variable of negative exponential distributed random process.

$$pdf(A) = \frac{2A}{\sigma^2} e^{\left(-A^2/\sigma^2\right)} \tag{2}$$

$$pdf(I) = \frac{1}{\sigma^2} e^{\left(-I/\sigma^2\right)} \tag{3}$$

From a statistical perspective, the multiplicative nature of amplitude and intensity data can be explained as follows. Consider two fixed, independent to σ unit distributions given below:

$$pdf(A_1) = 2A_1 e^{\left(A_1^2\right)} \tag{4}$$

$$pdf(I_1) = e^{\left(-I_1\right)} \tag{5}$$

It is then trivial to prove that amplitude and intensity are simply scaled versions of these unit variables, ie. $A = \sigma A_1$ and $I = \sigma^2 I_1$. These relationships evidently manifest a multiplicative nature. In fact, this condition has long been noted, but from different perspectives, in various SAR models including the multiplicative model [11] and product model [18].

If spatial homogeneity is defined as imaging scenes having the same back-scattering coefficient σ, then over a homogenous area, the measured values can then be considered as samples coming from a single stochastic process. Consequently, the population expected mean and variance of the four distributions are given in Table I.

From the above analysis, it is evident that amplitude as well as intensity SAR data suffer from hetoroskedastic phenomena, which is defined as the dependence of conditional expected variance of SAR data on the conditional expectation of the

TABLE I: Both the mean and the variance of original SAR data are related to the scale factor σ.

Mean	Variance
$avg(A_1) = \sqrt{\pi}/2$	$var(A_1) = (4-\pi)/4$
$avg(I_1) = 1$	$var(I_1) = 1$
$avg(A) = \sigma \cdot \sqrt{\pi}/2$	$var(A) = \sigma^2 \cdot (4-\pi)/4$
$avg(I) = \sigma^2$	$var(I) = \sigma^4$

TABLE II: Mean and Variance of Log Transformed values: here the variance is no longer dependent on σ

Mean	Variance
$avg(L_{1^A}) = \frac{-\gamma}{2} \cdot \frac{1}{\ln 2}$	$var(L_{1^A}) = \frac{\pi^2}{24} \cdot \frac{1}{(\ln 2)^2}$
$avg(L_{1^I}) = -\gamma \cdot \frac{1}{\ln 2}$	$var(L_{1^I}) = \frac{\pi^2}{6} \cdot \frac{1}{(\ln 2)^2}$
$avg(L_A) = \frac{-\gamma}{2} \cdot \frac{1}{\ln 2} + \log_2 \sigma$	$var(L_A) = \frac{\pi^2}{24} \cdot \frac{1}{(\ln 2)^2}$
$avg(L_I) = -\gamma \cdot \frac{1}{\ln 2} + 2\log_2 \sigma$	$var(L_I) = \frac{\pi^2}{6} \cdot \frac{1}{(\ln 2)^2}$

mean. In the context of speckle filtering, Table I indicates the vicious cycle: estimating variance is equal to estimating the mean and to estimating the unknown parameter σ, i.e. the main problem.

The formulas above have long been noted. In fact while pioneering the estimation of the equivalent number of looks (ENL) index, Lee et al commented that the ratio of expected standard deviation to mean is a constant in both cases (ie. $snr(A) = \sqrt{\frac{4}{\pi} - 1}$ and $snr(I) = 1$). Here, we just offer a different intepretation, which sets the stage for the discussion of logarithmic transformtion.

B. The effects of Heteroskedasticity on Speckle Filters

Even though the statistical model within individual resolution cells is well established, the applicability of its models is restricted to homogenous areas. Practical images, however, are heterogenous. Crucially it is this spatial variation that is of high interest. This fact gives rise to a question that seemed obvious: how to label an analysis area as being heterogenous and subsequently, what to do in the case of heterogeneity.

Various statistical models for heterogenous areas have been proposed (see [1] for a detailed review). Unfortunately, while most of the models highlight the multiplcative nature of sub-pixel or homogenous original SAR data, in extending the models to heterogenous images, virtually none have noted that spatial variation also gives rise to the heteroskedasticity phenomena. Heteroskedasticity, as explained in the previous section, is defined as the dependence of conditional expected variance of original SAR data on the conditional expectation of its mean, or equivalently its underlying back-scattering coefficient (σ). It is believed that this heteroskedasticity gives rise to serious negative impacts at various stages of speckle-filtering.

In modelling, heteroskedasticity has direct consequences to the central question of homogeneity or heterogeneity. In normal images, the contrast or variance among neighboring pixels is often used to measure homogeneity. Unfortunately such techniques do not appear to be effective under the heteroskedastic condition of original SAR data. In SAR images, both of these measures are dependent on the underlying coefficient (σ). This makes the problem of estimating variance to be equal to the problem of estimating the mean (i.e. equivalent to estimating σ).

Heteroskedasticity also poses numerous challenges in designing and evaluating an efficient estimator. Heteroskedasticity directly violates Gauss-Markov theorem's homoskedastic assumption. Thus it renders the efficiency of any naive Ordinary Least Square estimator [19], together with the normal Mean Squared Error evaluation criteria in serious doubt. If the variance is known *a priori*, it has been proven that a weighted mean estimator is the best linear unbiased estimator. Interestingly, as noted by Lopes [10], most known common successful adaptive filters [6] [7] [8] does make use of weighted mean estimators. However, the caveat is that in SAR speckle filtering, variance is not known *a priori*. And even though variance can be estimated from observable values, as the vicious circle goes, estimating the variance is as good as estimating the underlying coefficient σ itself.

A case in point is the recently improved sigma filter [20]. The technique determines outlying points as being too far away from the standard deviation. However, as is done in [20], to estimate standard deviation, an estimator of mean is required and used. It is interesting to note that the MMSE estimator used to estimate the mean in [20], itself alone, is a rather successful speckle-filter [6].

Last, but certainly not least is the bad impact of heteroskedastic on SAR image interpretation. Most of the task to be carried out in intepreting SAR images almost certainly involves target detection, target segmentation and/or target classification. Each of these tasks require good similarity or discriminant functions. Fundamental to these is the need of a consistent measures of distance. Unfortunately, by definition, heteroskedasticity leads to inconsistent measures of distance. This inconsistent measure of distance, coupled with the failure of the ordinary least square regression methods, are believed to cause a large class of artificial neural networks as well as a number of other computational intelligence methods for SAR classification to underperform.

C. Homoskedastic effect of Logarithmic Transformation

In this paper, we propose using a base-2 logarithmic transformation of orignal SAR data. Base-2 is chosen for implementation reasons since it can be computed faster than either natural or decimal logarithms, and yet maintains the ability to transform heterskedactic speckle into a homoskedastic relationship. Thus the original variables become:

$$L_1^A = \log_2(A_1) = L_1^I/2 \tag{6}$$
$$L_A = \log_2(A) = L_1^A + \log_2 \sigma \tag{7}$$
$$L_1^I = \log_2(I_1) = 2L_1^A \tag{8}$$
$$L_I = \log_2(I) = L_1^I + 2\log_2 \sigma \tag{9}$$

Bearing the relationship among the random variables in mind, it is then trivial to show that the probability distribution of these log-transformed variables are related as follows:

$$pdf(L_1^A)=2\cdot 2^{\left(2L_1^A\right)}e^{-2^{\left(2L_1^A\right)}} \quad (10)$$

$$pdf(L_A)=2\cdot 2^{(2L_A-2\log_2\sigma)}e^{-2^{(2L_A-2\log_2\sigma)}} \quad (11)$$

$$pdf(L_1^I)=2^{L_1^I}e^{-2^{L_1^I}} \quad (12)$$

$$pdf(L_I)=2^{(L_I-2\log_2\sigma)}e^{-2^{(L_I-2\log_2\sigma)}} \quad (13)$$

Noting that these distributions belong to the Fisher-Tippet family, the population expected mean and variances are obtained as in Table II, with $\gamma = 0.577$ being the Euler-Mascheroni constant. Most importantly, it can be seen that the means are biased and the variances are no longer related to σ

The equations above also highlight the relationships among random variables in the log-transformed domain. Two conclusions become evident from these formulae. Firstly, in the log-transformed domain, working on either amplitude or intensity will tend to give identical results. Secondly, the effects of converting the multiplicative nature to an additive nature through logarithmic transformation is clearly manifested. Table II confirms the condition of homoskedasticity, defined as the independence of the conditional expected variance on the conditional expectation of the mean. This result is consistent with findings by Arsenault [21]. The main difference would be the use of base-2 logarithm which is preferred here for more efficient computation.

Table III summarizes the discussion so far. It can be seen that while the original data, especially intensity values, should be preferred for multi-look processing, the log-transformed domain with its homoskedastic distribution offers consistent measures of dispersion and contrast. Thus log transformation is shown here to be a homomorphic transformation, allowing one to apply traditional linear, additive, least squared error regression signal processing (including wavelets) and computational (including artificial neural network) techniques on SAR data.

To verify this experimentally, Fig. 1 plots the histogram of observable data within a known homogenous area (from a RADARSAT2 image) against modelled PDF response. The excellent agreement is self-evident in the graph which confirmed the log-transformed model. In fact, this modelling has been used successful in explaining speckle phenomena, also verified through scientific experiments [22].

D. Consistent measures of distance in Log-Transformed domain

The consistent feature is explored and illustrated in this section from two different perspectives. First, we assume that the back-scattering coefficient σ is *known a priori*. With that, let us consider the dispersion random variable defined as the distance between an observable sample and its expected value:

$$D_A = A - avg(A) \quad (14)$$

$$D_I = I - avg(I) \quad (15)$$

$$D_{L^A} = L_A - avg(L_A) = log_2 A - log_2[avg(A)] \quad (16)$$

$$D_{L^I} = L_I - avg(L_I) = log_2 I - log_2[avg(I)] \quad (17)$$

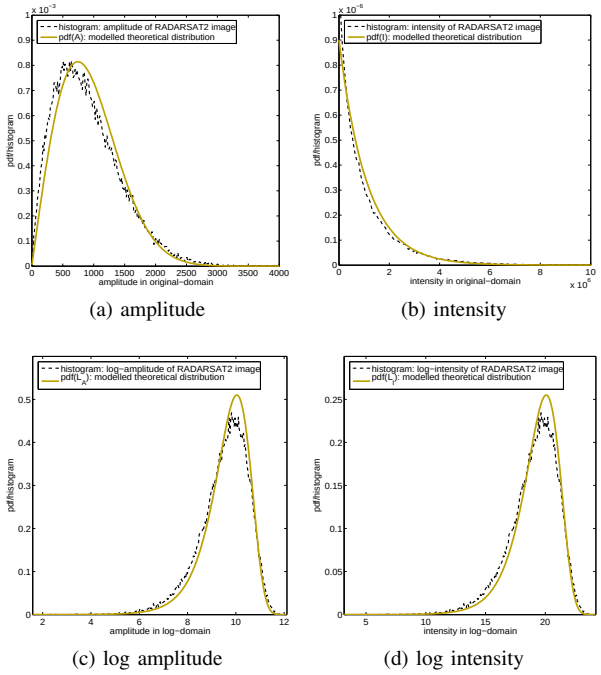

(a) amplitude (b) intensity

(c) log amplitude (d) log intensity

Fig. 1: Observed histogram in homogenous area and modelled pdf response

Noting the results from the previous section, the pdf for these variable can be derived as follows:

$$pdf(D_A) = 2\cdot\frac{(D_A+\sigma\sqrt{\pi}/2)}{\sigma^2}e^{\left[-\frac{(D_A+\sigma\sqrt{\pi}/2)^2}{\sigma^2}\right]} \quad (18)$$

$$pdf(D_I) = \frac{1}{\sigma^2}e^{\left[-(D_I+\sigma^2)/\sigma^2\right]} \quad (19)$$

$$pdf(D_{L^A})=2\cdot 2^{\left(2D_{L^A}+2\frac{\gamma}{2\ln 2}\right)}e^{-2^{\left(2D_{L^A}+2\frac{\gamma}{2\ln 2}\right)}} \quad (20)$$

$$pdf(D_{L^I})=2^{\left(D_{L^I}+\frac{\gamma}{\ln 2}\right)}e^{-2^{\left(D_{L^I}+\frac{\gamma}{\ln 2}\right)}} \quad (21)$$

From these equations, it is clear that these distributions, which are dependent on σ in the original domain, are now independent of it when processed in the log-domain.

Let us investigate SAR data from the second perspective, where two adjacent resolution cells are known to have *an identical but unknown* back-scattering coefficient σ. Now, the contrast random variable is defined, also in the log-transformed domain, as the distance between two measured samples.

$$C_A = A_1^\sigma - A_2^\sigma \quad (22)$$

$$C_I = I_1^\sigma - I_2^\sigma \quad (23)$$

$$C_{L^A} = L_1^{A_\sigma} - L_2^{A_\sigma} = log_2(A_1/A_2) \quad (24)$$

$$C_{L^I} = L_1^{I_\sigma} - L_2^{I_\sigma} = log_2(I_1/I_2) \quad (25)$$

Noting that $C_x = D_1^x - D_2^x$, it should come as no suprise that the measure of contrast is consistent in the log-domain but inconsistent in the original domain. The pdf of the log-transformed variables can be expressed as:

TABLE III: The properties of observable SAR random variables

RV	Relationships	Variance (skedasticity)	Mean (biasness)
A	$A = \sigma A_1$	Heteroskedastic $var(A) = \frac{(4-\pi)}{4} \cdot \sigma^2$	Unbiased $avg(A) = \frac{\sqrt{\pi}}{2} \cdot \sigma$
I	$I = A^2 = \sigma^2 I_1$	Heteroskedastic $var(I) = \sigma^4$	Unbiased $avg(I) = \sigma^2$
L_A	$L_A = \ln(A) = L_{1^A} + \log_2 \sigma$	Homoskedastic $var(L_A) = \frac{\pi^2}{24} \cdot \frac{1}{(\ln 2)^2}$	Biased $avg(L_A) = \frac{\gamma}{2} \cdot \frac{1}{\ln 2} + \log_2 \sigma$
L_I	$L_I = \ln(I) = L_{1^I} + 2\log_2 \sigma$	Homoskedastic $var(L_I) = \frac{\pi^2}{6} \cdot \frac{1}{(\ln 2)^2}$	Biased $avg(L_I) = \gamma \cdot \frac{1}{\ln 2} + 2\log_2 \sigma$

$$pdf(C_{L^A}) = 2 \frac{2^{(2C_{L^A})}}{\left[1 + 2^{(2C_{L^A})}\right]^2} \ln 2 \quad (26)$$

$$pdf(C_{L^I}) = \frac{2^{(C_{L^I})}}{\left[1 + 2^{(C_{L^I})}\right]^2} \ln 2 \quad (27)$$

Evidently these distributions are also consistent, i.e. they are independent of σ. To illustrate this property, Fig. 2 is generated by using data from the RADARSAT-2 image. As can be seen, it shows excellent agreement between the analytical pdf and the observable histogram of dispersion and contrast computed from an homogeneous area in the image.

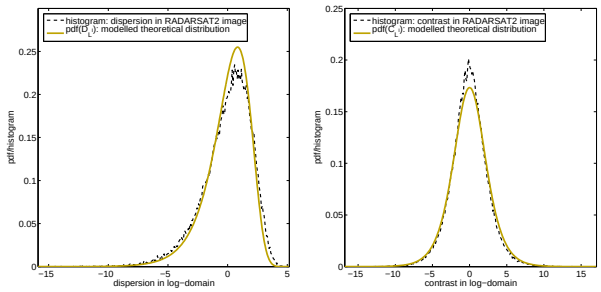

(a) dispersion (b) contrast

Fig. 2: Observed and modelled pdf of dispersion and contrast in homogenous log-transformed intensity images.

Given that real SAR images are heterogenous and the backscattering coefficient is unknown, it is evident that the measure of observable contrast in original SAR data differs, i.e. is inconsistent, across different homogenous areas. On the other hand, the observable contrast in the log-transformed domain is consistently the same across different homogenous areas. As such, one possible benefit is that should the sigma filter [20] be designed against the $pdf(C_{L^I})$, then the scale estimator would probably no longer be required.

E. Sampling distribution of Variance in Log-Transformed domain

From the results of the previous section, two sample variance distribution ($V_x = C_x^2$) can be given analytically as follows:

$$pdf(V_{L^I}) = \ln 2 \frac{2\sqrt{V_{L^I}}}{\sqrt{V_{L^I}} \left(1 + 2\sqrt{V_{L^I}}\right)^2} \quad (28)$$

$$pdf(V_{L^A}) = \ln 2 \frac{2\sqrt{4V_{L^A}}}{\sqrt{4V_{L^A}} \left(1 + 2\sqrt{4V_{L^A}}\right)^2} \quad (29)$$

It could be seen that, in the log-transformed domain, not only is the expected mean of the observable variance constant, the sampling distribution of this random variable is also independent of σ. While we have observed this analytically for variances based on two samples, for a larger number of samples, Monte-Carlo simulation can be used to visualise the PDF of samples' variances.

In summary, a few measurements of distance, being dispersion and contrast, are shown to agree with the consistent sense of variance and homoskedasticity. The dispersion measurement can be used to test if a pixel belongs to a "known" class of physical scatterer [23]. The consistent sense of contrast can be used to test if any pair of measured data points belong to the same homogeneous class. An example application of this is described in our fMLE speckle filter [24]. It may also explain why, in the original SAR domain, the ratio based detector / classifier is preferred to differential measures, which are not consistent. The consistent sense of contrast also gives rise to consistent measures of sample variances, which for example, can be used to test if a group of pixels can form a homogenous area. This was applied in a clustering algorithm described in [23].

F. Speckle Filtering Process And The Homoskedastic Log-transformed Domain

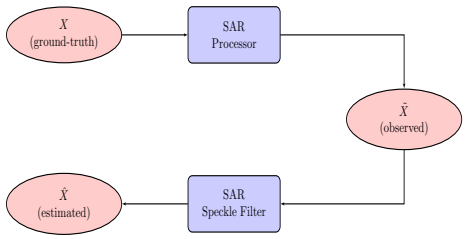

Fig. 3: SAR simulation, processing and filtering schema

Fig. 3 illustrates the general schema of SAR simulation / processing and SAR speckle filtering process. The "SAR processor" block indicates that either one of the following processes can occur. First is the normal process of SAR

processing where the unknown ground radiometric attribute (X) is recorded in $\tilde{X}$. Second is the simulation process where the noisy SAR data $\tilde{X}$ is simulated from a known ground-truth pattern X.

The "SAR Speckle Filter" block indicates the speckle filtering process, which takes the noisy speckled SAR data $\tilde{X}$ as input and outputs $\hat{X}$ as a better estimation of the ground-truth (i.e. X). The speckle filters used in this paper are: boxcar filter, enhanced Lee filter, enhanced Kuan filter, enhanced Frost filter, Gamma Map filter and PDE filter [25]. Evidently for the special case where there is no filter applied then $\hat{X}^{none} = \tilde{X}$.

Logarithmic transformation offers several consistent measures of distance, which is hypothised to be significant in evaluating speckle filters. A case in point is in visual evaluation of filtered results obtained from real captured SAR images. Since the radiometric ground-truth is not available, the most common way to evaluate speckle filters then is by qualitative visual evaluation. A conventional method is to investigate the ratio images between the filtered output and the noisy input images. Since logarithmic transformation converts these ratio into substractive residual which are consistent, residual analysis can be used to analyse and evaluate the performance of speckle filters. For visual comparison, Fig. 4 depicts the residual image in the log-transformed domain and the ratio images in the original domain, where a simple boxcar filter has been applied to data obtained from a real RADARSAT SAR image. "Visible" structure appears to be more easily discernable in the log-2 residual random pictures than in the ratio images, although this conclusion is of course itself a subjective one.

$$MSE_{true} = E\left[(\hat{X}^L - X^L)^2\right] \quad (30a)$$

$$MSE_{base} = E\left[(\tilde{X}^L - X^L)^2\right] \quad (30b)$$

$$MSE_{noise} = MSE_{residual} = E\left[(\hat{X}^L - \tilde{X}^L)^2\right] \quad (30c)$$

$$MSE_{benchmark} = |MSE_{residual} - MSE_{base}| \quad (30d)$$

As qualititative visual evaluation is subjective by nature, quantitative metrics and measurements are preferred, if relevant and possible. Different metrics to evaluate speckle filters, which will be investigated in subsequent sections, are given in Eqns. 30, all in log-transformed domain. When ground-truth is available, either in simulated experiments or over homogeneous area where it can be reasonably estimated, true MSE is the expected squared error between the estimated and true values.

However, in real captured SAR images where such ground truth is unknown, the evaluation can then be carried out through a benchmarked MSE. The idea is that since both the speckled values and the estimated values are available, the residual MSE_{noise} can be computed, which can be thought of as the level of noise being removed by speckle filtering process. Even as the ground-truth is not known in real SAR images, their speckle level (i.e. ENL) may be known or can be estimated reasonably well. Thus the base MSE level, which is also a measure of the speckle noise level, can also be estimated. Naturally, the speckle filter should remove as much noise as possible, while it also should not remove more variations than that caused by the speckle noise.

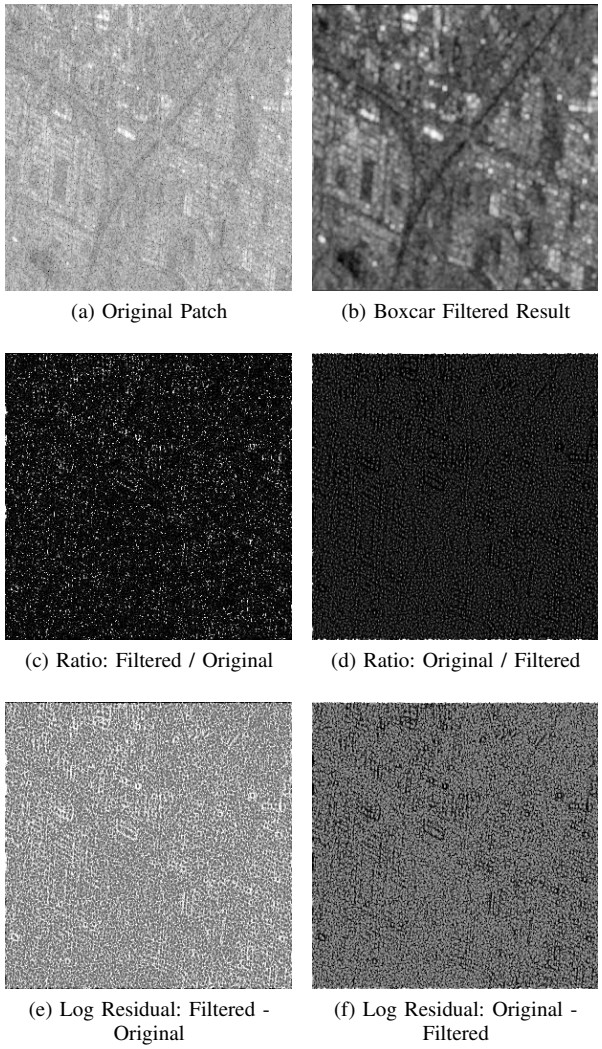

(a) Original Patch (b) Boxcar Filtered Result

(c) Ratio: Filtered / Original (d) Ratio: Original / Filtered

(e) Log Residual: Filtered - Original (f) Log Residual: Original - Filtered

Fig. 4: Visualising Removed "Noise": Ratio images in the original domain vs. Residual images in the log-transformed domain

IV. Evaluating Speckle Filters on Homogeneous Areas

In this section, a methodology to evaluate speckle filters over homogeneous area in the log-transformed domain is illustrated. Under the condition of homogeneity, speckle filters are supposed to estimate with negligible bias. Then the filters are traditionally compared by measuring their speckle suppression power using the ENL index. Consequently, in the log-transformed domain, the first component of MSE evaluation (i.e. bias evaluation) is probably insignificant in comparison to the other components, namely, variance evaluation. Subsection IV-A gives a theoretical justification for our methodology where variance methods of evaluation are shown to be mathematically related to the ENL index. The final subsection details how variance evaluation in the log-transformed domain to evaluate the levels of speckle over homogeneous areas.

A. Estimating ENL from MSE index in homogeneous areas

In this subsection, we show that the variance in the log-transformed domain can be related mathematically to the ENL index. Over homogeneous area, the ground-truth is unchanged, i.e. $X_i^L = X^L \forall i$. Assuming the filters achieve negligible bias, i.e. $E(\hat{X}^L) = X^L$, then the MSE evaluation is reducced to variance evaluation. That is, for known homogeneous scenes, MSE can be estimated as the observable variance of the filtered output in the log-transformed domain.

Let us consider the speckle suppression effect of multi-look processing in the log-transformed domain. Hoek [26] and Xie [27] have given the variance for L-look log-transformed random variables as:

$$var(\hat{X}^L) = \frac{1}{\ln^2(2)} \left(\frac{\pi^2}{6} - \sum_{i=1}^{L-1} \frac{1}{i^2} \right). \tag{31}$$

Taking results of the Euler proof for the Basel problem, we have $\frac{\pi^2}{6} = \sum_{i=1}^{\infty} \frac{1}{i^2}$, then $var(Y^L) = \frac{1}{\ln^2(2)} \left(\sum_{i=L}^{\infty} \frac{1}{i^2} \right)$. Noting that $\frac{1}{i} - \frac{1}{i+1} = \frac{1}{i(i+1)} < \frac{1}{i^2} < \frac{1}{i(i-1)} = \frac{1}{i-1} - \frac{1}{i}$, then $\frac{1}{L} - \frac{1}{\infty} < \sum_{i=L}^{\infty} \frac{1}{i^2} < \frac{1}{L-1} - \frac{1}{\infty}$. In fact, we could estimate:

$$var(\hat{X}^L) = \frac{1}{(L-0.5)\ln^2(2)} \tag{32}$$

Thus the ENL, i.e. L, can be estimated as:

$$\hat{L}_{est} = \frac{1}{var(\hat{X}^L)\ln^2(2)} + 0.5 \tag{33}$$

The above analysis can be verified experimentally. First, a 512×512 homogeneous area is generated and corrupted with single look SAR-speckle PDF. Different multi-look processing filters are then applied to the image patch. The observable variance in the log-transformed domain is recorded, and ENL is then estimated from Eqn. 33 for each simulation. The simulation is performed multiple times, with Table IV reporting the results in terms of mean and standard deviation. The theoretical variances are calculated from Equation 31, together with the analytical values from Eqn. 32. These experimental results evidently validate the analysis given above. They also shows that while the approximation in Eqn. 33 may not be perfect, since ENL is supposed to be an integer, the value obtained actually corresponds very closely with the nearest correct integer result.

The finding here may also help to explain other seemingly unrelated results. For example, Solbo [28] used standard deviation in the log-transformed domain to measure homogeneity, while Lopes [10] proposed the use of variation co-efficient index $C_v = std(I)/avg(I)$ to evaluate scene heterogeneity.

ENL	Var (Theory)	Var (Analysis)	Var (Observed)	$\hat{L}_{est}$
2	1.3423	1.3876	1.3452 (0.0031)	2.047 (0.0036)
3	0.8221	0.8326	0.8191 (4.2e-5)	3.041 (0.0001)
4	0.5907	0.5947	0.5941 (0.0059)	4.004 (0.0351)
5	0.4607	0.4625	0.4622 (0.0010)	5.003 (0.0099)
6	0.3774	0.3784	0.3800 (0.0009)	5.977 (0.0131)
7	0.3196	0.3202	0.3188 (0.0037)	7.029 (0.0769)
8	0.2771	0.2775	0.2786 (0.0002)	7.970 (0.0065)
9	0.2446	0.2449	0.2455 (0.0007)	8.979 (0.0244)
10	0.2189	0.2191	0.2183 (0.0012)	10.035 (0.0538)
11	0.1981	0.1982	0.1975 (0.0001)	11.038 (0.0063)
12	0.1809	0.1809	0.1810 (0.0022)	12.001 (0.1419)
13	0.1664	0.1665	0.1661 (0.0002)	13.031 (0.0191)
14	0.1541	0.1542	0.1534 (0.0016)	14.068 (0.1387)
15	0.1435	0.1435	0.1432 (0.0019)	15.036 (0.1967)
16	0.1342	0.1343	0.1342 (0.0009)	16.006 (0.0987)
17	0.1261	0.1261	0.1249 (0.0005)	17.159 (0.0636)
18	0.1189	0.1189	0.1192 (0.0010)	17.959 (0.1406)
19	0.1125	0.1125	0.1126 (0.0004)	18.976 (0.0788)
20	0.1067	0.1067	0.1074 (0.0005)	19.889 (0.0937)
21	0.1015	0.1015	0.1017 (0.0002)	20.975 (0.0357)
22	0.0968	0.0968	0.0970 (0.0002)	21.952 (0.0337)
23	0.0925	0.0925	0.0924 (0.0006)	23.027 (0.1386)
24	0.0886	0.0886	0.0887 (0.0002)	23.957 (0.0507)
25	0.0849	0.0849	0.0846 (0.0007)	25.094 (0.1934)

TABLE IV: Speckle Suppression Power: ENL and Variance

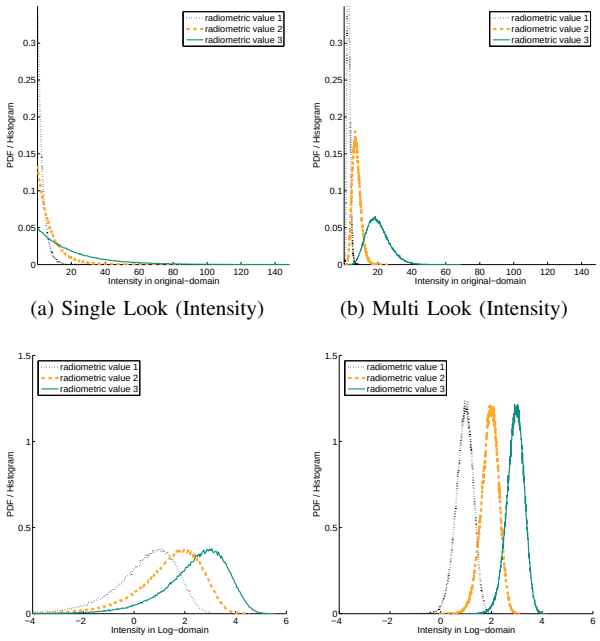

(a) Single Look (Intensity) (b) Multi Look (Intensity)

(c) Single-Look in Log Domain (d) Multi-Look in Log Domain

Fig. 5: The Inconsistency evident in the original SAR domain and the Emerged Consistency demonstrated in the log-transformed domain

B. Using log-variance to evaluate speckle filters

Fig. 5 plots the histograms of homogenous SAR data over different radiometric values. Both single-look simulated and multi-look processed/box-car filtered data is displayed. Specifically the plots show that the log-transformed domain is consistent while the plots from the original domain are not.

Fig. 6 shows that all of the standard filters (Lee, Kuan, Frost and Gamma MAP) preserve this consistency in their filtered output. Intuitively, as the boxcar filter is actually similar to multi-look processing, thus its output also does exhibit the this consistency. This consistency will also lead to the consistent sense of distance described earlier, which is significant because it is the tell-tale indicator of the consistent contrast and variance. This ensures applicability of various target detection/classification algorithms which employ statistical properties in the un-filtered data, such as the ratio based discriminator in the original domain or the differential based discriminator in the log-transformed domain.

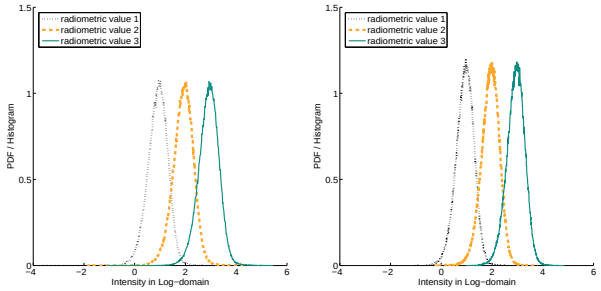

(a) Lee filter

(b) Kuan Filter

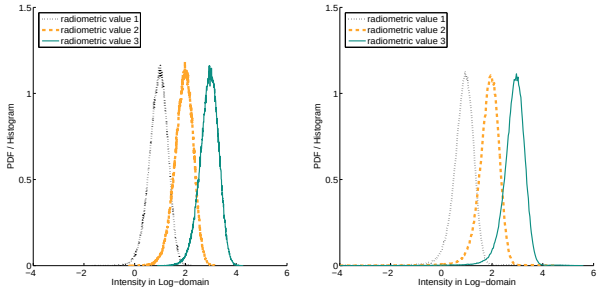

(c) Frost Filter

(d) Gamma MAP filter

Fig. 6: Filtered results: consistency in log-transformed domain

Filter	Set	Log-Variance	$\hat{L}_{est}$	Avg Intensity
none	1	3.4149 (0.0003)	1.1095 (5.8e-5)	3.4795 (0.0029)
pde	1	1.2674 (0.0014)	2.1423 (0.0018)	3.4806 (0.0029)
map	1	1.2651 (0.0055)	2.1454 (0.0072)	3.1627 (0.0002)
lee	1	0.4604 (0.0027)	5.0206 (0.0268)	3.4835 (0.0022)
kuan	1	0.2979 (0.0024)	7.4864 (0.0574)	3.4748 (0.0054)
frost	1	0.2852 (0.0012)	7.7975 (0.0299)	3.4799 (0.0027)
boxcar	1	0.2513 (0.0011)	8.7819 (0.0353)	3.4799 (0.0027)
none	2	3.4191 (0.0068)	1.1088 (0.0012)	9.4925 (0.0049)
pde	2	1.6071 (0.0026)	1.7952 (0.0021)	9.4930 (0.0048)
map	2	1.2646 (0.0023)	2.1459 (0.0029)	8.6091 (0.0162)
lee	2	0.4653 (0.0026)	4.9731 (0.0254)	9.4936 (0.0080)
kuan	2	0.2999 (0.0026)	7.4391 (0.0602)	9.4761 (0.0014)
frost	2	0.2867 (0.0005)	7.7595 (0.0128)	9.4912 (0.0039)
boxcar	2	0.2532 (0.0006)	8.7203 (0.0193)	9.4914 (0.0040)
none	3	3.4203 (0.0187)	1.1068 (0.0033)	25.6234 (0.0389)
pde	3	2.0353 (0.0021)	1.5226 (0.0010)	25.6236 (0.0389)
map	3	1.2799 (0.0091)	2.1263 (0.0116)	23.2628 (0.0304)
lee	3	0.4633 (2.4e-5)	4.9926 (0.0002)	25.6406 (0.0488)
kuan	3	0.2964 (0.0010)	7.5225 (0.0244)	25.6112 (0.0226)
frost	3	0.2862 (0.0008)	7.7714 (0.0202)	25.6263 (0.0409)
boxcar	3	0.2529 (0.0005)	8.7296 (0.0178)	25.6261 (0.0407)

TABLE V: Filters' Performance: Homogeneous Area

Table V provides a quantitative comparison among the filters. It shows that the filters can all preserve the underlying radiometric values, while their speckle suppression power can be equivalently measured using either variance in the log-transformed domain, or the standard ENL index.

V. Evaluating Speckle Filters on Heterogenous Area

In this section, the MSE criteria (MSE_{true}) is validated through experiments and analysis. From a statistical estimation framework point of view, the use of MSE to evaluate statistical estimators is natural. Because the log-transformation converts heteroskedastic SAR speckle into a homoskedastic distribution model, the log-transformed domains MSE is much preferred to MSE in the original SAR domain. Experimentally, on clear-cut simple target-background patterns, the results that follow will indicate that the lower the MSE achievable by a speckle filter, the better the feature preservation performance recorded for its output.

The general requirements of feature preservation, for simple scenes with only targets and clutter, can be broken down into the requirements of radiometric preservation and speckle suppression. In the log-transformed domain, these smaller requirements are equivalent to the bias and variance evaluation of statistical estimators. Overall, while the MSE index combines the measurements of bias and variance evaluation, the feature preservation requirement, in the context of simple target and clutter scenes, can be measured by the standard metric for target detectability: the Area Under the ROC Curve (AUC). We show experimentally that MSE inversely correlates with the AUC index, for each of the simulated patterns.

Since the filters are expected to be consistently behaved in the log-transformed domain, as we repeat a pattern multiple times, the histograms of the target and background areas can be reliably obtained. The target and background can then be seperated using a simple threshold based classification model. The separability of the two stochastic populations are judged by the standard ROC, and the quantitative and normalized metric of AUC can then be used as an evaluation metric.

The types of test pattern used in this paper include the followings: point targets, line targets, edge targets and a heterogeneous checker board. These test patterns could of course be concatenated into a larger composite test image, although we will consider them as separate images to allow easier analysis of the results. Each pattern comprises two classes of ground-truth: background and target areas. We follow the convention used in the radar community where the target is signified by the brighter area of the image. Fig 7 shows a small section (32×32 window) of each pattern.

Large patches of these patterns (512×512) are first corrupted with single look speckle. The filters are then applied onto these noised images. From a high-level perspective, Fig. 8 shows that feature preservation can be evaluated by examining the separability of the two background and target populations. Subfigures 8c and 8d allows visual evaluation of target and clutter histograms and their separability. Quantitative evaluation of these separability is carried out by plotting the Receiver Operating Curve (ROC), in subfigures 8e and 8f respectively, and is measured by computing the Area Under these Curves (AUC).

Detailed examination of figures 8 and 9 can help to explain how the MSE is related to the histograms' separation capability. In pre-filtered images, shown in subfigures 8c and 9c, there is no bias error visible. Then the seperability of clutter and target populations depends only on the variance of the additive noise. This variance is visualized as the horizontal spread of the histograms. Naturally, given a fixed location (i.e. expectation) of the two populations, the smaller the spread (i.e. variance), the better the separation capability.

In post-filtered images, shown in subfigures 8d and 9d,

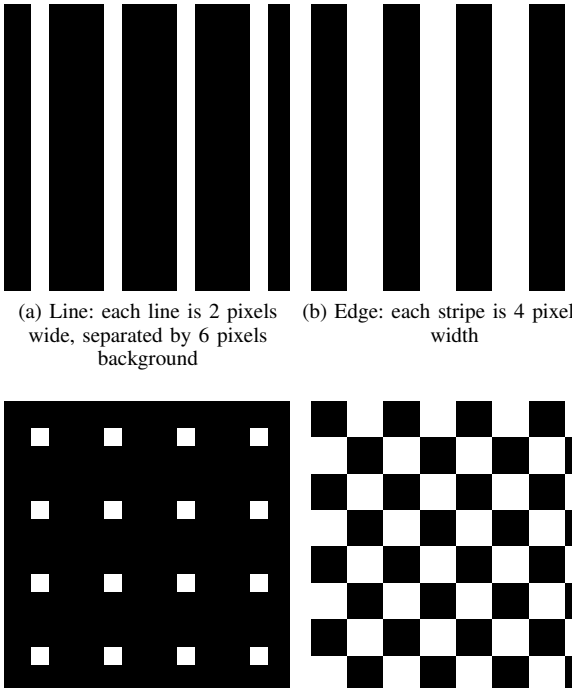

(a) Line: each line is 2 pixels wide, separated by 6 pixels background

(b) Edge: each stripe is 4 pixels in width

(c) Point: each point is a 2×2 square spacing 6 pixels apart

(d) Checker board: the squares are 4 pixels wide each side

Fig. 7: Example windows of ground truth patterns, each 32×32 pixels in size.

the situation is more complicated. Here, besides the effect of the histogram spread, one also needs to take into account the bias error. Close investigation of subfigure 9d indicates that the output of the Kuan filter, and in fact the outputs of all other filters (which are not reproduced here due to space constraints), also introduce bias errors. Specifically, the target (brighter) populations are always under-estimated and the clutter (darker) population are always over-estimated. This is probably due to the entropy reduction effect of the speckle filters. Apparently, assuming that the variances are fixed, the lower these bias errors, the better the separation capability.

Thus, the MSE performance of the estimator, which combines the effect of bias and variance error, can be used to evaluate the separability of the two histograms. Table VI provides the measurements of MSE and AUC performance for various filters and patterns. It shows that the MSE is inversely correlated to this separability index. The first column in Table VII quantitatively measures this statistical correlation. The results suggest that the lower MSE achievable by the filters would, in general, lead to better feature preservation.

VI. Using MSE to find the most suitable speckle filter for practical SAR images

In this section, our conjecture of using MSE in the log-transformed domain to find the most suitable speckle filter for practical real-captured SAR images is described. In these scenarios, the ground-truth, and hence the true MSE, is not available. Therefore, only the residential MSE is computable. Assuming the level of speckle noise (i.e. ENL or MSE_{base}) is

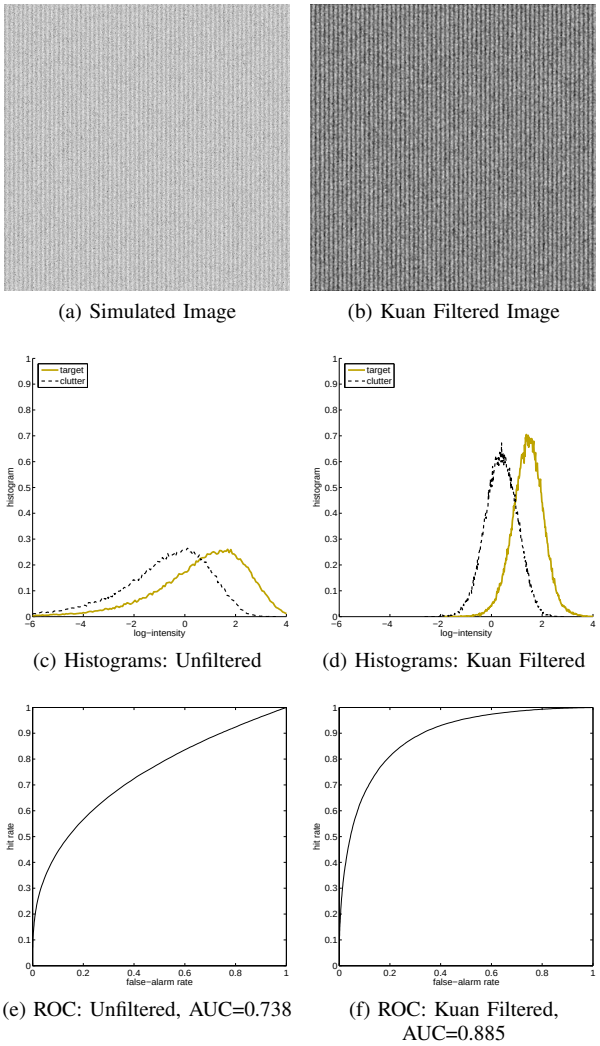

(a) Simulated Image

(b) Kuan Filtered Image

(c) Histograms: Unfiltered

(d) Histograms: Kuan Filtered

(e) ROC: Unfiltered, AUC=0.738

(f) ROC: Kuan Filtered, AUC=0.885

Fig. 8: Target and Clutter Separability: Histograms and resulting ROC Curve visualisation

known or can be estimated, then the benchmark MSE is also measurable. Our heuristic rule is that the best filtered results are those that have minimal benchmarked MSE. This heuristic rule allow us to choose the "best" filtered results from an array of standard speckle filters for a captured SAR image, where the ground-truth and hence true MSE is not available. Intuitively, the hypothesis is that the best speckle filter for a given scene is the one having its removed variation being closest to the inherent speckle noise.

Experimental results are presented as empirical evidence supporting the conjecture. The experiments in the previous sections are repeated on single-look SAR images which are simulated from given ground-truth aerial images. Then the filters are applied onto the simulated SAR images. Fig. 10 illustrates some of the images used for our experiments.

With the use of MSE being validated from previous experiments, the most suitable filter can be considered as the one with the lowest true MSE. Table VIII shows that among the various filters used, the most suitable filter is also the filter that has its observable residual MSE value being closest to

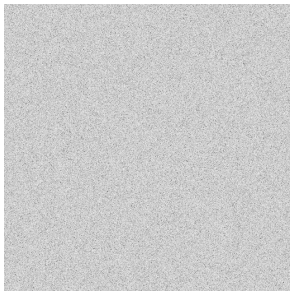

(a) Error Image: Unfiltered

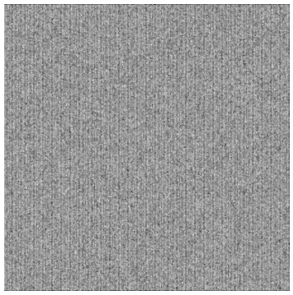

(b) Error Image: Kuan Filtered

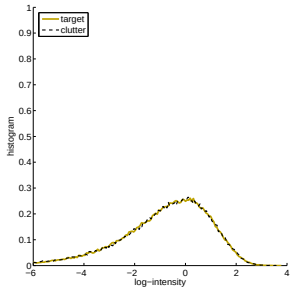

(c) Error Histograms: Unfiltered

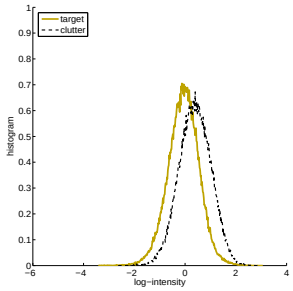

(d) Error Histograms: Kuan-filtered

Fig. 9: Bias Error Investigation: Image and Histogram Visualisation

Pattern	Filter	AUC	MSE_{true}	MSE_{noise}
point	unfiltered	0.741 (0.7e-3)	4.101 (1.3e-3)	2e-33 (4e-36)
point	pde	0.789 (1.3e-3)	1.291 (5.1e-3)	1.817 (2.2e-3)
point	map	0.813 (1.4e-3)	1.679 (2.2e-3)	2.183 (7.4e-3)
point	frost	0.836 (1.8e-3)	0.536 (2.4e-3)	4.976 (6.9e-3)
point	lee	0.857 (0.9e-3)	0.615 (3.1e-3)	3.189 (0.9e-3)
point	boxcar	0.871 (1.5e-3)	0.471 (1.7e-3)	4.503 (5.4e-3)
point	kuan	0.882 (1.1e-3)	0.448 (2.3e-3)	3.859 (3.4e-3)
edge	unfiltered	0.738 (1.5e-4)	4.128 (9.0e-3)	2e-33 (1e-35)
edge	pde	0.783 (0.6e-4)	1.409 (0.3e-3)	1.589 (0.4e-2)
edge	map	0.830 (0.6e-4)	1.712 (3.5e-3)	2.184 (0.8e-2)
edge	frost	0.841 (0.6e-4)	0.551 (0.1e-3)	5.035 (1.3e-2)
edge	boxcar	0.871 (0.2e-4)	0.486 (0.2e-3)	4.560 (1.3e-2)
edge	lee	0.872 (0.7e-4)	0.619 (2.2e-3)	3.233 (1.3e-2)
edge	kuan	0.885 (0.4e-4)	0.471 (2.0e-3)	3.909 (1.1e-2)
checker	unfiltered	0.738 (4.5e-4)	4.11 (7.8e-3)	2e-33 (5e-36)
checker	pde	0.785 (6.2e-4)	1.445 (2.6e-3)	1.586 (2.4e-3)
checker	map	0.836 (4.0e-4)	1.663 (1.1e-3)	2.213 (4.6e-3)
checker	frost	0.855 (5.6e-4)	0.528 (2.2e-3)	4.965 (9.3e-3)
checker	lee	0.879 (2.2e-4)	0.605 (1.7e-3)	3.229 (2.8e-3)
checker	boxcar	0.883 (6.4e-4)	0.466 (2.4e-3)	4.493 (9.1e-3)
checker	kuan	0.894 (4.2e-4)	0.453 (0.9e-3)	3.860 (9.5e-3)
line	unfiltered	0.737 (1.1e-3)	4.129 (7.3e-3)	2e-33 (6e-36)
line	pde	0.752 (1.2e-3)	1.339 (2.0e-3)	1.885 (3.7e-3)
line	map	0.801 (1.6e-3)	1.706 (5.8e-3)	2.188 (3.5e-3)
line	frost	0.831 (1.3e-3)	0.551 (1.1e-3)	5.023 (0.5e-3)
line	lee	0.847 (1.5e-3)	0.623 (2.9e-3)	3.228 (4.8e-3)
line	boxcar	0.865 (1.3e-3)	0.486 (0.9e-3)	4.549 (0.9e-3)
line	kuan	0.874 (1.9e-3)	0.464 (1.9e-3)	3.897 (4.9e-3)

TABLE VI: Lower MSE suggest better feature detection, measured by the AUC index

Pattern	AUC - MSE_{true}	AUC - $MSE_{benchmark}$
edge	-0.8958 (1.5e-05)	-0.9778 (1.6e-09)
point	-0.9012 (1.1e-05)	-0.9816 (5.3e-10)
checker	-0.9077 (7.3e-06)	-0.9829 (3.5e-10)
line	-0.8223 (3.1e-04)	-0.9421 (4.8e-07)

TABLE VII: The correlation between MSE and AUC evaluation criteria (inside the brackets are corresponding p-values)

(a) A Rural Area in Vietnam

(b) A Suburb of Ha Noi

Fig. 10: Ground Truth Images for simulation

Pattern	Filter	MSE_{true}	MSE_{noise}
Vietnam rural	none	4.1174	4e-35
Vietnam rural	pde	3.8022	0.0368
Vietnam rural	lee	0.4984	3.2555
Vietnam rural	frost	0.3490	4.6856
Vietnam rural	kuan	0.3396	3.6877
Vietnam rural	boxcar	0.3107	4.2328
Hanoi suburb	none	4.1321	4e-35
Hanoi suburb	pde	3.8004	0.0391
Hanoi suburb	lee	0.5261	3.2598
Hanoi suburb	frost	0.3811	4.7427
Hanoi suburb	kuan	0.3619	3.7270
Hanoi suburb	boxcar	0.3395	4.2882

TABLE VIII: If the best filters are the ones with smallest true MSE, then their observable noise-MSE are also the ones closest to the MSE of inherent noise

the noise MSE (4.1167 in the case of this example). The conjecture is also validated using visual evaluation, an example of which is presented in Fig. 11.

The results from the experiments in previous sections can also be used to validate the use of residual and benchmark MSE. The AUC-$MSE_{benchmark}$ column in Table VII shows that the criteria index is strongly correlated with feature classification capability, measured by the standard AUC index.

The conjecture is also validated in real SAR images. Different speckle filters are applied onto a real RADARSAT-2 image. In this case, since the ground-truth is not available, only visual evaluation can be used to validate our conjecture. Table IX tabulates the computed MSE of the "removed" additive noise. Evidently all filters still leave some noise "unremoved", in which case, the higher removed noise MSE would probably suggest a more suitable filter. Fig. 12 tends to confirm this visually.

Filter	$MSE_{residual}$	$MSE_{benchmark}$
pde	0.2583	3.8584
map	2.6936	1.4231
kuan	3.3924	0.7243
lee	3.4172	0.6995
boxcar	3.6918	0.4249
frost	4.1191	0.0024
none	MSE_{base}	4.1167

TABLE IX: Our Conjecture: Most Suitable Speckle Filter For The Scene Can Be Chosen Using The Residual MSE.

(a) Ground-Truth Image

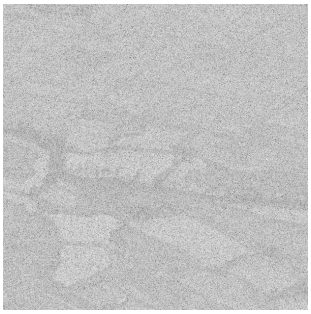

(b) Unfiltered Image
$MSE_{true} = MSE_{base} = 4.1174$

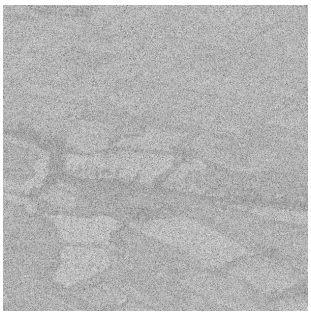

(c) PDE Result: $MSE_{true} = 3.8022, MSE_{noise} = 0.0073$

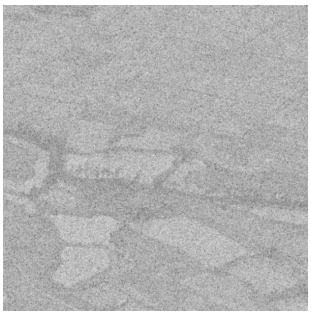

(d) Lee Result: $MSE_{true} = 0.4984, MSE_{noise} = 3.25553$

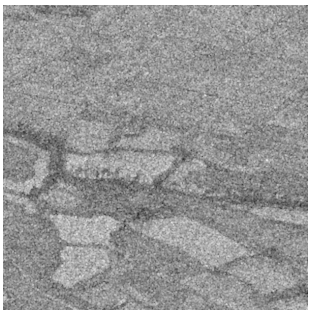

(e) Frost Result: $MSE_{true} = 0.3490, MSE_{noise} = 4.6856$

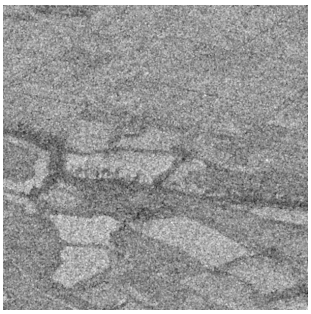

(f) Boxcar Result: $MSE_{true} = 0.3107, MSE_{noise} = 4.2328$

Fig. 11: Filtering Simulated Real Images: Qualititative Validation

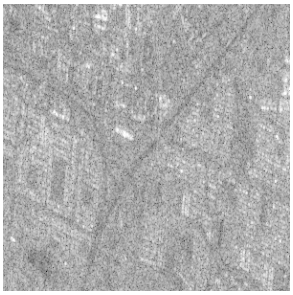

(a) PDE Filter:
$MSE_{benchmark} = 3.8584$

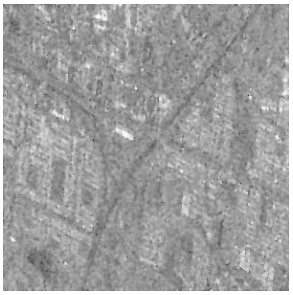

(b) MAP Filter:
$MSE_{benchmark} = 1.4231$

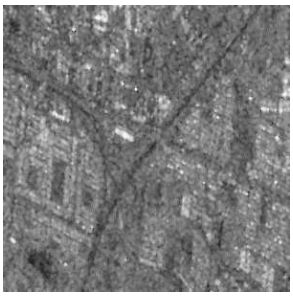

(c) Lee Filter:
$MSE_{benchmark} = 0.6995$

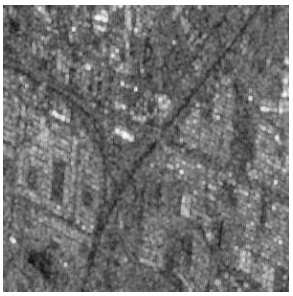

(d) Frost Filter:
$MSE_{benchmark} = 0.0024$

Fig. 12: Filtering Real Images: Smaller $MSE_{benchmark}$ suggests visually better images

VII. Discussion and Conclusion

A. Discussion

Although it is widely known that log transformation transforms multiplicative SAR speckle into additive noise, one should note that the noise is not Gaussian. In fact, figures presented in the previous sections show that they are not even centered around the origin. This may explain why averaging filters in the log-transformed domain (e.g. [21]) do not work very well in practice. To counter this, the use of maximum likelihood estimation, instead of simple averaging, is suggested [24]. Interestingly, averaging is also the MLE operator in the SAR's original domain.

Log transformation also brings about a few consistent measures of dissimilarity. This consistency can be found in single-look or multi-look SAR data, as well as in filtered outputs of various "standard" speckle filters. This allows a variety of target detection/classification algorithms - which exploit these consistent statistical properties - to not only perform brilliantly on pre-filtered data, but also be found practically working on post-filtered data.

These consistent measures of distance in the log-transformed domain could probably have implications beyond speckle filtering. For example, in the subsequent tasks of designing target detectors or classifiers, it is normally desirable for the solution to work on both unfiltered and post-filtered SAR data. In such cases, these consistent dissimilarity measures found in the log-transformed domain could provide a sound theoretical basis. In fact, a number of proposed solutions have already appeared to exploit this feature. A case in point is the simple ratio based discriminator in the original SAR domain. Looking backwards, in designing new speckle filters, by ensuring that the filtered output preserves these consistent properties, the newly designed filters would be eligible to be employed as pre-processing step for properly designed classifiers / detector. From a higher level perspective, the applicability of Gauss-Markov theorem and consequently a meaningful MSE predict fruitful applications for a variety of least-squared-error algorithms in the homoskedastic log-transformed domain.

Of course, there are other speckle filters that do not preserve such consistency (e.g. the PDE filter [25]). One could argue that it would not be fair to judge such filters using the MSE criteria, which tend to favour the "standard" filters. While we respect any other criteria that have been used, we reiterate the

two salient points of our approach. Firstly, our MSE criteria is closely related to the basic ENL criteria. As shown in previous sections, experimental results indicated that the ENL measures for such filter (i.e. the PDE filter) differ depending on the radiometric values. Secondly, speckle filters need to serve a purpose, and evaluation criteria should be relevant to such purpose. The MSE criteria is shown to be related to feature preservation requirements. Thus it is relevant towards subsequent target detection / classification processing, believed to be a common subsequent processing step. For these two reasons, the MSE criteria is advocated.

In the experiments above, speckle filters with a 3×3 sliding window were used even though we are aware that the normal window size employed is much larger. The reasons for maintaining such a small window is that smaller-sized filters facilitate the use of smaller patterns without too much concern for crosstalk among adjacent targets. In addition, we focused on the use of MSE in the log-transformed domain for the evaluation of speckle filters, and do not wish to advocate any particular "best" filter. In other words, we addressed the methodology of evaluating speckle filters, and did not directly address the design of speckle filters. However, interested filter designers are invited to download the open Matlab source code used in this paper for evaluating their own designs [1].

In this paper, stochastic simulation is used extensively to evaluate the performance of statistical estimators (i.e. speckle filters). The use of small and simple patterns allows detailed analysis which can then be done repeatedly and reliably against the stochastic nature of SAR data. This also helps in mapping qualitative requirements for the speckle removal process into specific and quantitative requirements in the design of speckle filters. Its use also provides an absolute ground-truth as a solid base for comparison of results across different papers.

The main drawback, of course, is that ground truth often does not exist in real-captured SAR images. Thus the result extension towards real images is only analogical. While the proposed rule is heuristic, the experimental results presented in this paper are shown empirically to be valid.

We distinctively divided speckle filtering into two distinct scenarios, that of homogeneity and heterogeneity. While perfect homogeneous ground truth can be defined, different heterogeneous patterns exhibits different levels of heterogeneity. As such, different measures have been proposed to evaluate heterogeneity levels. Unfortunately, for real captured images, where the absolute ground-truth is not available, there is no known and certain way to assert a given image as being perfectly homogeneous or absolutely heterogeneous. Thus while the distinction helps in clarifying the concepts, it is probably a leaky abstraction.

The patterns used are chosen based on our experience, which may affects evaluation results. As different patterns result in different homogeneity/heterogeneity degrees, they also appear to affect the performance and ranking of each speckle filters. One extreme example is that of perfect homogeneity, where boxcar filters would exhibit a respectable performance. While, at the other end of the spectrum: that of high heterogeneity, it is common knowledge that the boxcar filter would not perform that well.

The current scheme of finding the most suitable speckle filter requires the application of all filters before a decision is made, which probably demands excessive processing. A possibly better alternative would be to predict the choice, escaping such massive requirements of computational power. This, however, is outside the scope of this paper.

B. Conclusion

To summarise, speckle filters are generally evaluated using many different qualitative criteria. To compare the filters against each other, a methodology is needed to quantify these qualitative requirements, and subsequently to measure, compare and evaluate these quantities in the filtered results. Central to all these is the need for a consistent sense of distance.

Logarithmic transformation has been shown not only to convert multiplicative and heteroskedastic noise in the original SAR domain to additive and homoskedastic values, but also to offer a few consistent measures of distance. With the Gauss-Markov theorem becoming applicable in this domain, we describe and propose the use of MSE in the log-transformed domain as a unifying criteria to quantitatively measure different requirements for speckle filters.

Our contribution is mainly centered around a few points. Firstly, a mathematical equation is established to link the ENL index to the variance in the log-transformed domain. We also illustrate the use of log-variance evaluation - which is shown to be equivalent to the standard ENL evaluation - in evaluating the speckle suppression effect of different speckle filters. Secondly we show that MSE is inversely correlated to the AUC index for simulated heterogeneous areas. The result suggests that the smaller MSE a filter could achieve, the better it would be at discriminating between the underlying radiometric features. Thirdly, the practical contribution is to suggest an heuristic rules using the benchmark MSE to find the most suitable speckle filter for any given scene. Combined, we propose the use of MSE in log-transformed domain in evaluating the performance of different speckle filters in a variety of evaluation scenarios, and suggest several evaluation methodologies that may be useful in this regard.

It should also be noted that similar consistent measures of distance also exist in polarimetric SAR (POLSAR) data. Thus future work may explore the applicability of MSE approaches to POLSAR data analysis and processing.

[1] This can be found at `http://www.lintech.org/Hai/Matlab`

REFERENCES

[1] R. Touzi, "A review of speckle filtering in the context of estimation theory," *IEEE Transactions on Geoscience and Remote Sensing*, vol. 40, no. 11, pp. 2392 – 2404, Nov 2002.

[2] C. Oliver and S. Quegan, *Understanding Synthetic Aperture Radar Images*. SciTech Publishing, 2004.

[3] F. Medeiros, N. Mascarenhas, and L. Costa, "Evaluation of speckle noise MAP filtering algorithms applied to SAR images," *International Journal of Remote Sensing*, vol. 24, no. 24, pp. 5197–5218, Dec 2003.

[4] X. Wang and H. Sun, "An evaluation for speckle filters of SAR images," in *Society of Photo-Optical Instrumentation Engineers (SPIE) Conference Series*, vol. 6043, Nov 2005, pp. 761–766.

[5] Z. Shi and K. Fung, "A Comparison of Digital Speckle Filters," in *Proceedings of 1994 International Geoscience and Remote Sensing Symposium (IGARSS)* , 1994, pp. 2129–2133.

[6] J. Lee, "Digital image enhancement and noise filtering by use of local statistics," *IEEE Transactions on Pattern Analysis and Machine Intelligence*, vol. 2, pp. 165–168, Mar 1980.

[7] D. T. Kuan, A. A. Sawchuk, T. C. Strand, and P. Chavel, "Adaptive noise smoothing filter for images with signal-dependent noise," *IEEE Transactions on Pattern Analysis and Machine Intelligence*, vol. PAMI-7, no. 2, pp. 165 –177, Mar 1985.

[8] V. S. Frost, J. A. Stiles, K. S. Shanmugan, and J. C. Holtzman, "A model for radar images and its application to adaptive digital filtering of multiplicative noise," *IEEE Transactions on Pattern Analysis and Machine Intelligence*, vol. PAMI-4, no. 2, pp. 157 –166, Mar 1982.

[9] A. Lopes, E. Nezry, R. Touzi, and H. Laur, "Maximum A Posteriori Speckle Filtering And First Order Texture Models In SAR Images," in *Proceedings of the 1990 International Geoscience and Remote Sensing Symposium, 1990 (IGARSS)*, May 1990, pp. 2409 –2412.

[10] A. Lopes, R. Touzi, and E. Nezry, "Adaptive speckle filters and scene heterogeneity," *IEEE Transactions on Geoscience and Remote Sensing*, vol. 28, no. 6, pp. 992 –1000, Nov 1990.

[11] J.-S. Lee, "Speckle analysis and smoothing of synthetic aperture radar images," *Computer Graphics and Image Processing*, vol. 17, no. 1, pp. 24 – 32, 1981.

[12] L. Gagnon and A. Jouan, "Speckle filtering of SAR images - A comparative study between complex-wavelet-based and standard filters," in *Proceedings of The Society of Photo-optical Instrumentation Engineers (SPIE)*, vol. 3169, 1997, pp. 80–91.

[13] B. Oliver, "Sparkling spots and random diffraction," *Proceedings of the IEEE*, vol. 51, no. 1, pp. 220 – 221, Jan 1963.

[14] E. Leith, "Quasi-holographic techniques in the microwave region," *Proceedings of the IEEE*, vol. 59, no. 9, pp. 1305 – 1318, Sep 1971.

[15] J. W. Goodman, "Some fundamental properties of speckle," *Journal of the Optical Society of America*, vol. 66, no. 11, pp. 1145–1150, 1976.

[16] ——, "Statistical properties of laser speckle patterns," in *Laser Speckle and Related Phenomena*. Springer Berlin / Heidelberg, 1975, vol. 9, pp. 9–75.

[17] J.-S. Lee and E. Pottier, *Polarimetric Radar Imaging: From Basics to Applications*. CRC Press, 2009.

[18] E. Jakeman, "On the statistics of k-distributed noise," *Journal of Physics A: Mathematical and General*, vol. 13, no. 1, p. 31, 1980.

[19] M. Furno, "Comparison of estimators for heteroskedastic models," *Journal of Statistical Computation and Simulation*, vol. 38, no. 1, pp. 99 – 107, 1991.

[20] J.-S. Lee, J.-H. Wen, T. Ainsworth, K.-S. Chen, and A. Chen, "Improved Sigma Filter for Speckle Filtering of SAR Imagery," *IEEE Transactions on Geoscience and Remote Sensing*, vol. 47, no. 1, pp. 202 –213, Jan 2009.

[21] H. H. Arsenault and G. April, "Properties of speckle integrated with a finite aperture and logarithmically transformed," *Journal of the Optical Society of America*, vol. 66, no. 11, pp. 1160–1163, 1976.

[22] F. Ulaby, T. Haddock, and R. Austin, "Fluctuation statistics of millimeter-wave scattering from distributed targets," *IEEE Transactions on Geoscience and Remote Sensing*, vol. 26, no. 3, pp. 268 –281, May 1988.

[23] T. H. Le, I. V. McLoughlin, K. Y. Lee, and T. Brestchneider, "SLC SAR speckle filtering using homoskedastic features of logarithmic transformation," in *Proceedings of the 31th Asian Conference on Remote Sensing (ACRS)*, Hanoi, Vietnam, Nov 2010.

[24] T. H. Le and I. V. McLoughlin, "SAR Fuzzy-MLE speckle filter using the distance consistency property in homoskedastic log-transformed domain," in *Proceedings of the 32th Asian Conference on Remote Sensing (ACRS)*, Taipei, Taiwan, Nov 2011.

[25] Y.-L. You and M. Kaveh, "Fourth-order partial differential equations for noise removal," *IEEE Transactions on Image Processing*, vol. 9, no. 10, pp. 1723 –1730, Oct 2000.

[26] D. Hoekman, "Speckle ensemble statistics of logarithmically scaled data," *IEEE Transactions on Geoscience and Remote Sensing*, vol. 29, no. 1, pp. 180 –182, Jan 1991.

[27] H. Xie, L. Pierce, and F. Ulaby, "Statistical properties of logarithmically transformed speckle," *IEEE Transactions on Geoscience and Remote Sensing*, vol. 40, no. 3, pp. 721–727, Mar 2002.

[28] S. Solbo and T. Eltoft, "Homomorphic wavelet-based statistical despeckling of SAR images," *IEEE Transactions on Geoscience and Remote Sensing*, vol. 42, no. 4, pp. 711–721, Apr 2004.